Tribology and Materials
Vol. 3, No. 3, 2024, pp. 131-140 ISSN 2812-9717
https://doi.org/10.46793/tribomat.2024.015

# Friction and wear behaviour of AlCrN and TiN coated H13 tool steel

**Ben Samuel JOHNY** [1], **Mathew ALPHONSE** [2,*]

[1] C.S.I Institute of Technology, Thovalai, India
[2] Vel Tech Rangarajan Dr. Sagunthala R&D Institute of Science and Technology, Chennai, India
*Corresponding author: drmathew@veltech.edu.in

**Keywords**

H13 tool steel
pin-on-disc
TiN
AlCrN
SEM
AFM

**History**

Received: 03-08-2024
Revised: 23-09-2024
Accepted: 29-09-2024

**Abstract**

The wear characteristics of coated H13 tool steel and as-casted H13 tool steel in dry sliding conditions were investigated through a pin-on-disc tribometer, where the H13 steel is used as a pin and EN31 steel is used as disc material. The study was focused on evaluating the tribological behaviour by examining the friction characteristics, surface morphology and wear performance. Initially, to improve the hardness of the untreated (as-casted) H13 steel, the tempering process where carried out on the samples, which helped elevate the hardness from 38 to 55 HRC. The worn surface of the samples was analysed using atomic force microscopy (AFM). Among the four samples (as-casted, heat-treated, AlCrN coated and TiN coated) the as-casted samples were affected by oxidation and adhesive wear. The material loss measured for as-casted, heat-treated, AlCrN and TiN samples was 30.34, 7.85, 0.78 and 0.14 mg, respectively. The measured coefficient of friction was 0.541 for as-casted, 0.492 for the heat-treated, 0.48 for the AlCrN and 0.147 for the TiN sample. From the study, the major conclusion was that the TiN coating offers major wear protection and lower friction.

## 1. Introduction

In recent years, for protecting solid surfaces, coatings have found an essential place in major industries like aerospace, automotive, manufacturing and cutting tools, as well as in the biomedical sector [1-2]. The H13 tool steel is used in the industry for its wear resistance and toughness, which leads to the expanded life of the material. The H13 steel is unique because of its properties, such as heat resistance, toughness, machinability and corrosion resistance. H13 steel is mainly used in cutting tool applications [3-6]. The H13 steel can be coated, which enhances its friction properties, thermal fatigue and abrasion resistance [7-10]. Liquid and plasma nitriding were used for the in-depth investigation of the tribological and mechanical properties of the coated H13 steel samples. Notably, the wear resistance and roughness were improved [11-14]. Researchers are focused on finding various types of coating deposition methods for H13 steel substrate, which will be highly efficient in high-stress industry applications [15-18].



Telasang et al. [19] studied the magnetron sputtering method. They reported that coatings like AlCrFe and AlCrN are intricately structured, offering various advantages like wear and corrosion resistance. Chayeuski et al. [20] reported that coatings like titanium nitride (TiN) and diamond-like carbon (DLC) significantly improve the material's hardness and wear resistance. DLC and TiN coating also helps in improving the toughness and bonding between the surfaces and improves tool life. Vinoth et al. [21] have investigated the use of DLC coating which has improved wear of the coated surfaces and resulted in lower maintenance. Mishra et al. [22] have examined the surface of WC/Co material. The surface of the samples was coated with AlTiN and AlCrN, respectively. The test results were compared with as-casted steel, and results indicated a 30 % improvement in wear behaviour. In another study, Arrabal et al. [23] found that alloys can be better protected using coatings like plasma electrolytic oxidation, which may help in reducing wear by up to 30 %, increase the surface hardness, decrease porosity and lower coefficients of friction under applied load. In another study, TiC and TaC are included in the substrate of a TiAlN coated sample, which leads to the improvement of wear performance. It is noticed that this inclusion helps in increasing sample hardness and reduces the wear rate. Also, a formation of uniform microstructure was visible, which led to an improvement in the adhesion strength [24].

This study aims to focus on choosing a better coating for drilling tools. The H13 tool steel was chosen based on its low cost and good hardenability, and it is essential to analyse its wear behaviour. The tribological analysis was compared with heat-treated H13 tool steel and with TiN and AlCrN coated H13 tool steel.

## 2. Experimental procedure

The untreated (as-casted) H13 steel samples were prepared in a cylindrical form dimension. The dimensions were prepared based on the pin-on-disc instrument, i.e. for pin a 32 mm height and 8 mm diameter and for disc a 4 mm thickness and a 32 mm diameter. The chemical composition of the H13 steel is shown in Table 1.

**Table 1.** Chemical composition of H13 steel

| Element | C | Si | Mn | Cr | Mo | V | Fe |
|---|---|---|---|---|---|---|---|
| wt. % | 0.38 | 1.1 | 0.4 | 5.0 | 1.4 | 1.0 | Balance |

Before the coating deposition, the samples were heat-treated to improve the hardness [25-26]. It is important to improve the hardness of the H13 steel sample, which is measured using a Rockwell hardness tester. The applied load and the indenter penetrated during testing were 150 kg and 0.18 mm, respectively. Initially, the hardness measured for the as-casted steel was 38.10 HRC. At different stages, the samples were preheated to improve their hardness using a vacuum heat treatment process. The samples were preheated three times at 650, 850 and 1030 °C, followed by high-pressure nitrogen quenching and finally the samples were tempered at 1040 °C. The hardness values obtained from the Rockwell hardness (HRC) test of all samples are shown in Table 2.

**Table 2.** Rockwell hardness (HRC) of tested samples

| Sample | As-casted | Heat-treated | AlCrN coating | TiN coating |
|---|---|---|---|---|
| HRC | 38.10 | 53.01 | 79.12 | 78.02 |

The samples underwent a preparation process to ensure they were ready for coating deposition before the wear study. Using waterproof abrasive papers, successive grinding was processed, followed by polishing. Finally, ultrasonic cleaner was used to remove the residual impurities.

The samples for TiN coating deposition were placed in the vacuum chamber. Using magnetron sputtering or electric arc the titanium (100 %) target is vaporised to release titanium atoms. During the process, nitrogen gas is introduced in the vacuum chamber to form a titanium nitride (TiN) and the deposition rate was controlled for uniform thickness. During the process, the deposition rate for TiN coating is maintained at 0.1 micrometres per hour, the temperature is controlled at 450 °C and pressure is maintained at 1000 Pa. Similarly, for AlCrN coating, 50 % aluminium and 50 % chromium target is vaporised using magnetron sputtering or arc evaporation. By the nitrogen gas, which is introduced into the chamber, the aluminium and chromium atoms form aluminium chromium nitride (AlCrN). The deposition rate was controlled for uniform thickness. During the process, the deposition rate for AlCrN coating is maintained at 0.45 micrometres per hour, the temperature is controlled at 550 °C and pressure is maintained at 1000 Pa. The samples were cooled at room temperature to avoid thermal stress. The coating thickness observed during deposition was 3 and 3.5 µm for TiN and AlCrN, respectively.

The schematic image of the pin-on-disc tribometer is shown in Figure 1a, and the H13 steel sample mounted on the tribometer is shown in Figure 1b. Input parameters like speed, load and temperature are critical to ensuring quality products. The proper parameters result in less wear, minimising material wastage and improving productivity [26]. Based on a literature survey, the parameters used were as follows: sliding distance of 1200 m, sliding speed of 2 m/s, sliding diameter of 30 mm, sliding time of 10 minutes and a normal load of 40 N (0.796 MPa) [27,28]. The experiment where performed at a temperature of 250 °C and the disc speed of 1273 rpm was calculated based on the input parameters.

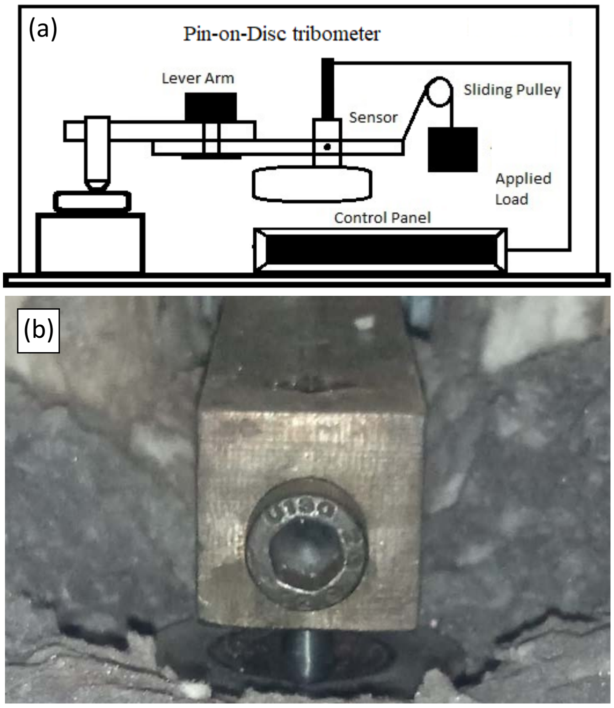


**Figure 1.** Pin-on-disc tribometer: (a) schematic image and (b) H13 mounted sample

The morphology and structure of the worn surface were analysed with a scanning electron microscope (SEM) equipped with a Zeiss Inca energy-dispersive X-ray spectroscopy (EDS) analyser and Nanosurf C3000 used for analysing the atomic force microscopy (AFM).

## 3. Results and discussion

### 3.1 Wear performance

The wear behaviour of the H13 steel was investigated by measuring the mass losses and analysing the surface morphology. Figure 2 shows the wear of the tested samples. The as-casted sample showed the highest wear among the tested samples of 30.34 mg, while the heat-treated and coated samples showed less wear. The coated samples (TiN and AlCrN) have less wear because of their higher hardness and thermal stability. Notably, the TiN coating showed improved wear resistance and reduced friction compared to the AlCrN coating. Table 3 shows the wear and coefficient of friction (CoF) values obtained during the test.

**Table 3.** Wear and friction results

| Sample | Wear, mg | CoF |
|---|---|---|
| As-casted | 30.34 | 0.541 |
| Heat-treated | 7.85 | 0.492 |
| AlCrN coating | 0.78 | 0.480 |
| TiN coating | 0.14 | 0.147 |

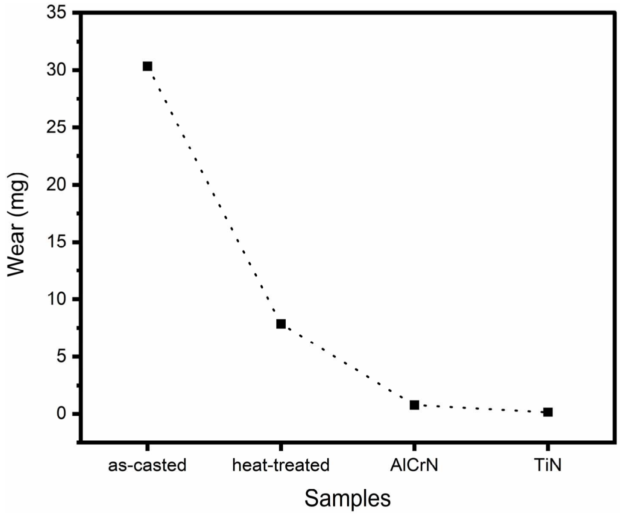


**Figure 2.** Wear of the tested samples

### 3.2 Coefficient of friction

The coefficient of friction (CoF) encompasses both, the statics and kinetic factors which govern the contact mechanisms among the surfaces. The higher CoF denotes an increase in resistance, which directly affects the life of the surface, optimal lifespan and performance [29,30]. Figure 3 shows the CoF images of the four tested samples, where the red line indicates the displacement of the probe in a horizontal direction during testing and the white line indicates the CoF.

The as-casted sample has the highest CoF of 0.541, while the minimum CoF was noticed for the TiN coated sample of 0.147. The wear was significantly lower for the TiN and AlCrN coated samples compared to the as-casted sample. These coatings have reduced surface irregularities, leading to the wear resistance.

### 3.3 Surface morphology

Figure 4 shows the surface morphologies of the tested samples after the test. Deep pits are noticed in the wear track region and slight peeling is present. The surface morphologies of the as-casted and heat-treated samples' worn region are shown in Figures 4a and 4 b. Fine scratches were observed near the edges of the wear region. Fewer oxides are visible on the wear surface area. This characterises oxidative and adhesive wear. No severe peeling has been observed in Figures 4c and 4d, i.e. on the worn surface of AlCrN and TiN coating. It is proved that the impact of temperature was minimal on coated samples, except in some spalling noticed on the AlCrN coated sample. At the as-casted sample, due to the

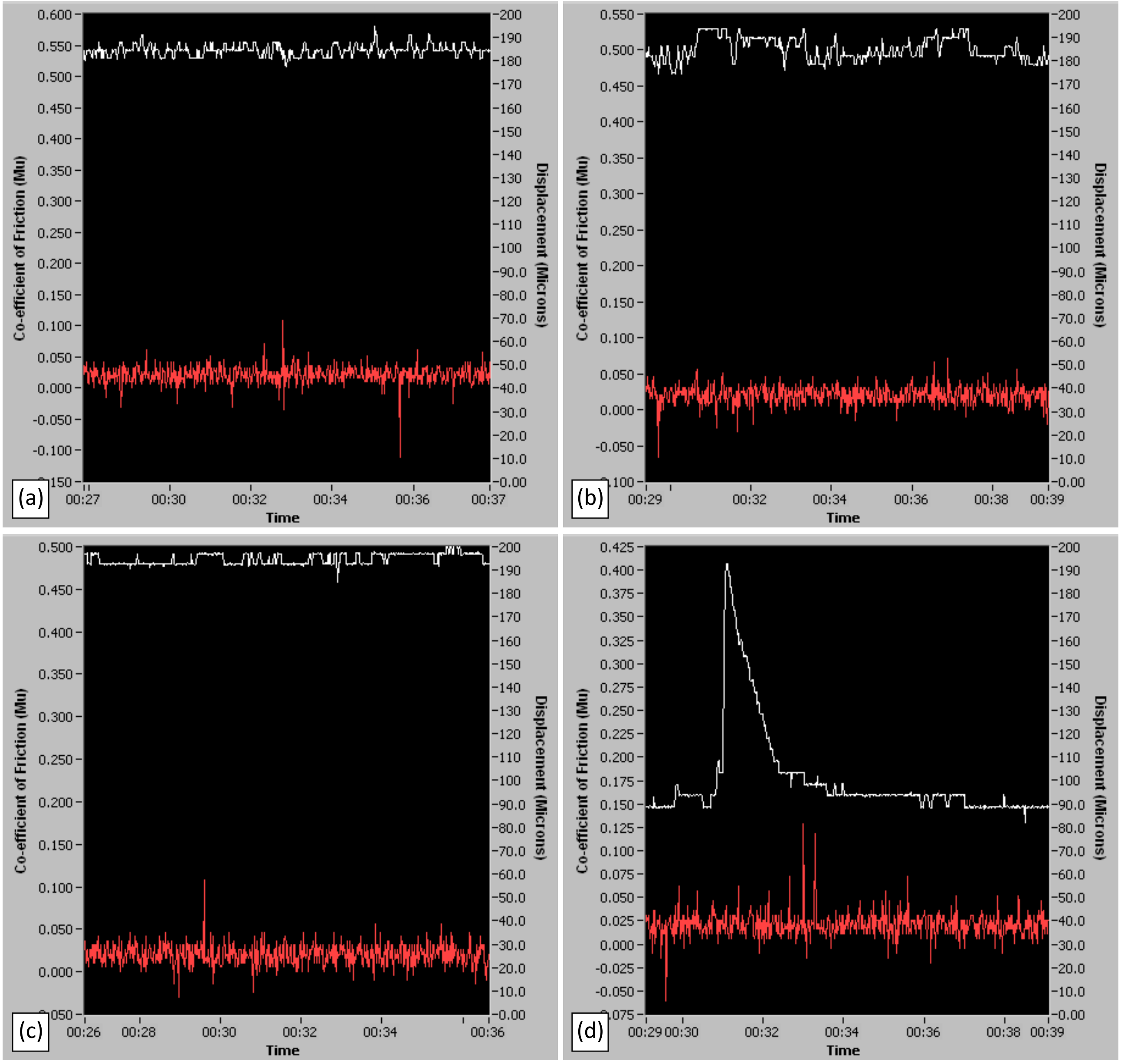


**Figure 3.** CoF images of tested samples: (a) as-casted, (b) heat-treated, (c) AlCrN coated and (d) TiN coated

continuous formation of fresh debris, the wear patterns are anticipated to worsen over time, which contributes to increased wear.

Furthermore, it is also noticed that there are significantly fewer irregularities in the coated samples when compared with other samples. However, the AlCrN coated sample shows a slight growth of irregularities and in the TiN coated sample, the surface became finer. The fine surface leads to uniform coating thickness and also enhances surface characteristics which further leads to enhanced wear resistance.

### 3.4 Energy-dispersive X-ray spectroscopy

Figure 5 shows the composition of the worn surface of tested samples. Figure 5a shows the traces of Fe and O, where Fe is observed more. The presence of adhesive wear is defined as a primary wear mechanism. It also has shown some delamination regions and cracks. Figure 5b shows the presence of high oxygen content, particularly in the worn area. Oxides were not detected on the coated samples' unworn surfaces, which resulted in their better surface finish (Figs. 6a and 6c). The content of Fe was lower in coated samples' worn surfaces, which also gives a better surface finish (Figs. 6b and 6d). From Figure 6b it could be seen that the surface reacted with oxygen, which may form an oxide layer. In as-casted sample, they are formed as thin layers which may not help prevent wear. Only adhesive wear is visible in the coated samples and oxidation wear is presented only in the as-casted and heat-treated samples.

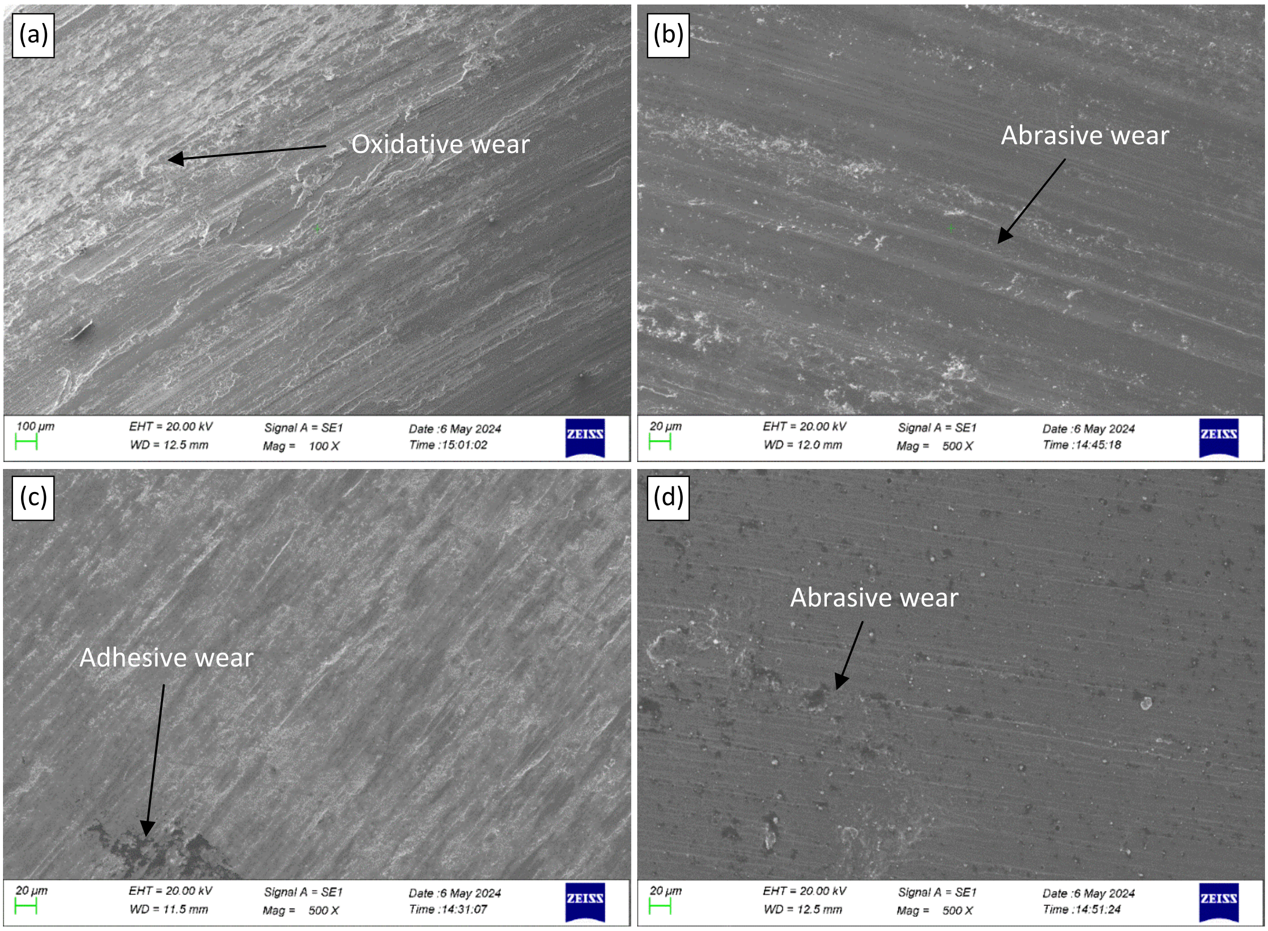


**Figure 4.** Surface morphologies of tested samples: (a) as-casted, (b) heat-treated, (c) AlCrN coated and (d) TiN coated

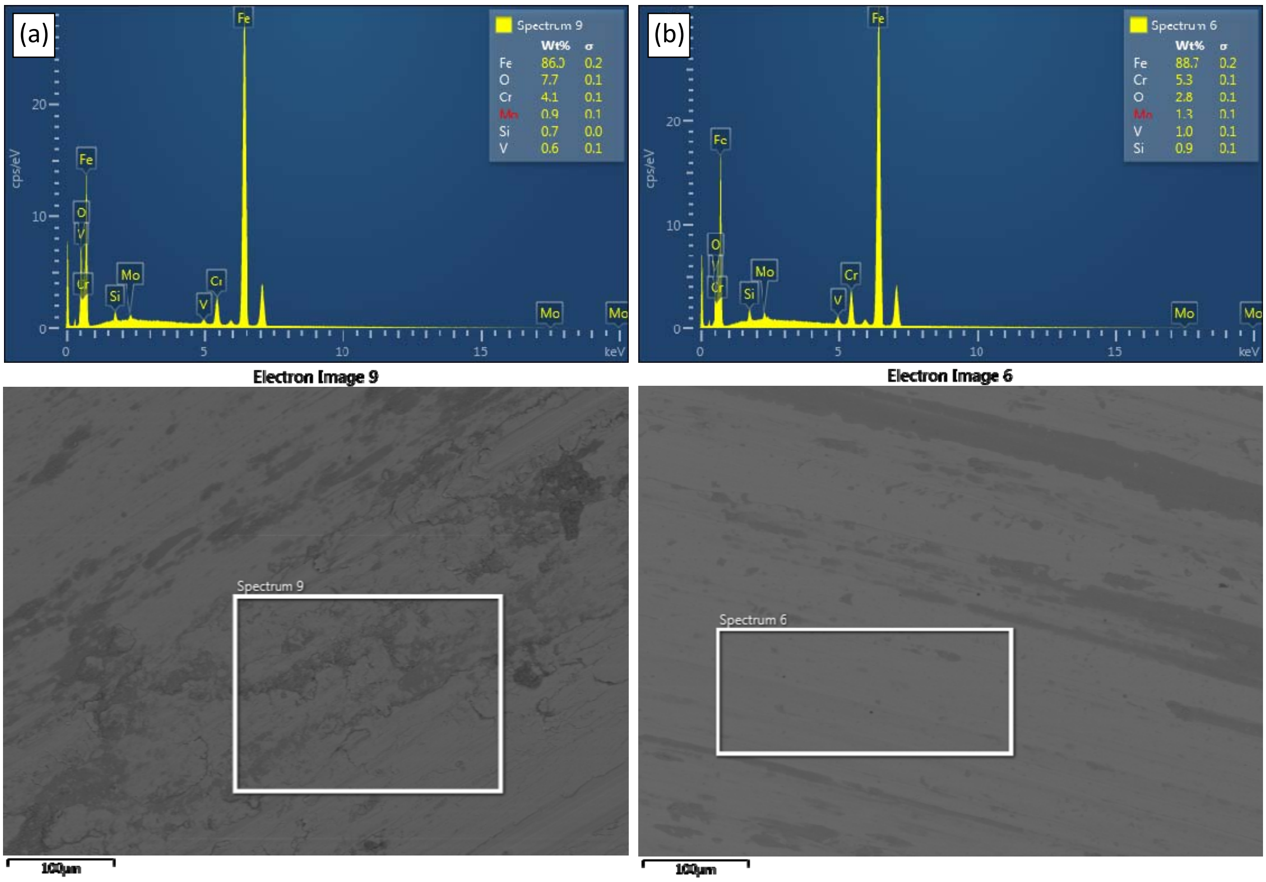


**Figure 5.** Composition of the worn surface of tested samples: (a) as-casted and (b) heat-treated

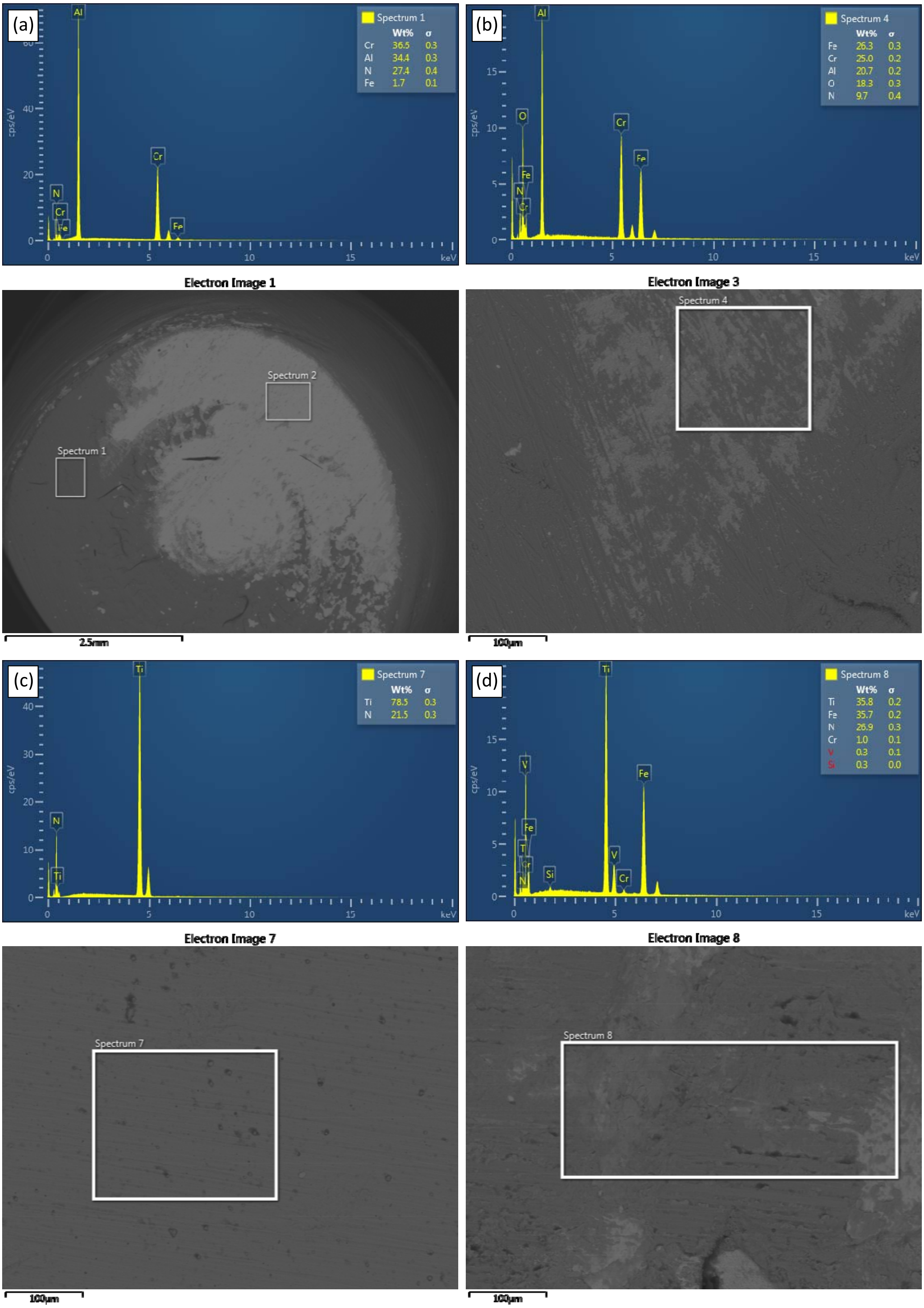


**Figure 6.** Composition of the unworn and worn surface of tested samples: (a) AlCrN coated (unworn), (b) AlCrN coated (worn), (c) TiN coated (unworn) and (d) TiN coated (worn)

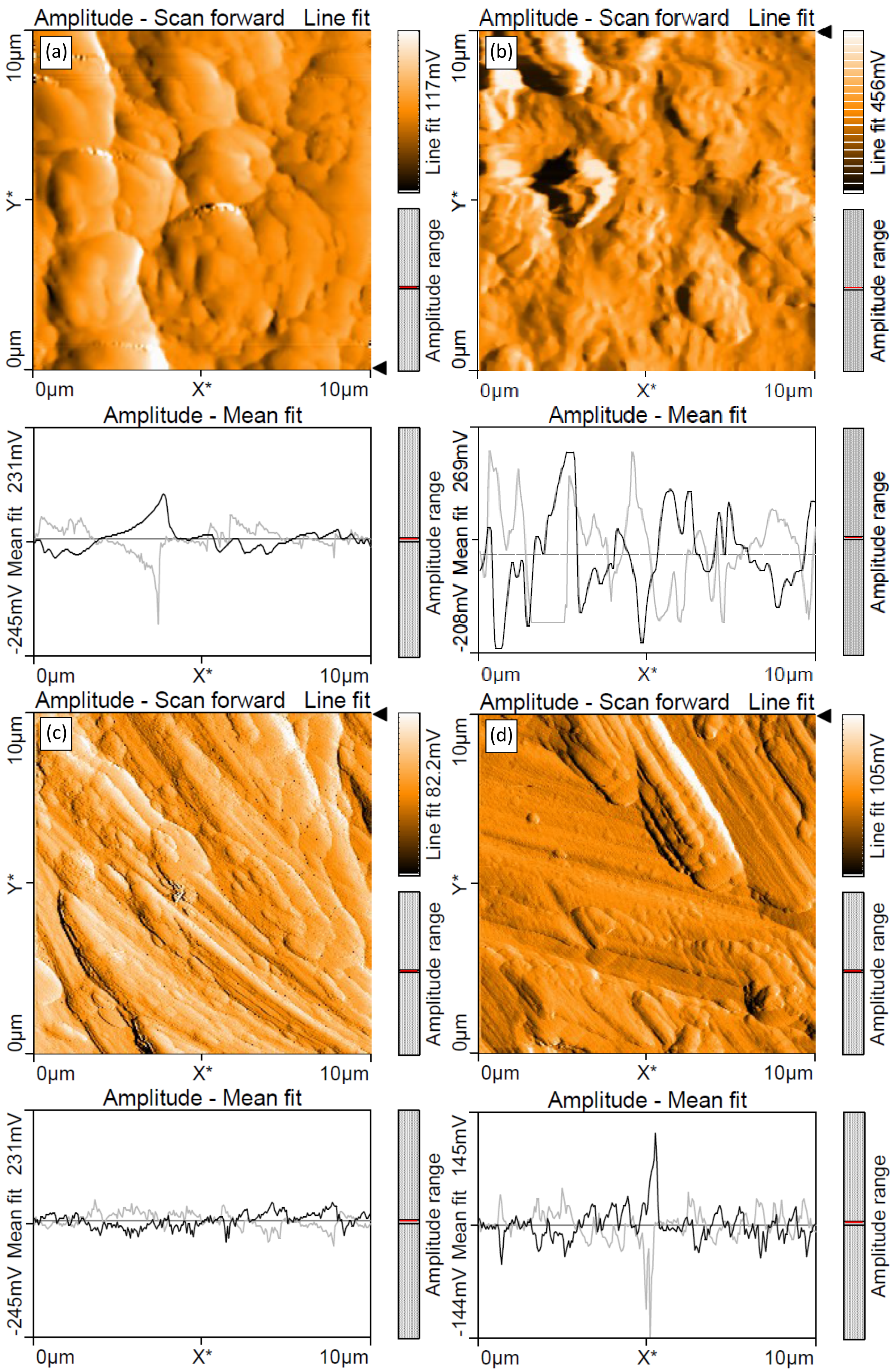


**Figure 7.** Surface roughness (2D model and graph obtained by AFM) of the samples: (a) as-casted, (b) heat-treated, (c) AlCrN coated and (d) TiN coated

### 3.5 Surface topography

The surface topography and roughness of the samples were studied, capturing them using atomic force microscopy (AFM). The AFM images help understand the visual representation of the samples' wear-induced topographical changes along the height values of the *z*-axis as shown in Figure 7. In the study, the image is captured over the worn surface area.

The area roughness parameters of the surface obtained by AFM are shown in Table 4. The parameters are defined as *Sa* (arithmetical mean height), *Sq* (root mean square height), *Sp* (maximum peak height) and *Sz* (maximum height).

**Table 4.** Area surface roughness obtained by AFM

| Parameter | As-casted | Heat-treated | AlCrN coating | TiN coating |
|---|---|---|---|---|
| *Sa*, nm | 158.94 | 169.26 | 164.69 | 72.631 |
| *Sq*, nm | 192.69 | 211.25 | 199.03 | 87.404 |
| *Sp*, nm | 592.88 | 792.19 | 479.26 | 262.43 |
| Sz, nm | 1106.1 | 1687.8 | 1053.8 | 532.48 |

Figure 7 illustrates the surface roughness of the samples as the 2D model and graph. The images reveal the existence of coating layers. The roughness of the heat-treated sample was higher than the as-casted sample, so the heat-treated sample showed better wear resistance due to its higher hardness. The AlCrN and TiN coatings (Figs. 7c and 7d) exhibited less roughness when compared with the heat-treated sample.

Due to the formation of a dense layer on the surface, the surface is free from delamination and makes the surface durable. Due to the crack's formation in the heat-treated sample, oxides form on the surface and layers peel off. Because of this, the roughness is higher at this sample. Surface damages (cracks) are noticed only on the surface of the heat-treated sample and very little damage on the as-casted sample.

## 4. Conclusion

The investigation was conducted to examine the friction value and wear resistance for the four samples, with the following conclusions.

For as-casted and heat-treated samples, oxidation wear and adhesive wear were noticed. The wear rates of AlCrN and TiN coatings are lower than those of the other two samples, while the TiN coating exhibited lower wear than the AlCrN coating. The wear was reduced by 99.5 % for TiN coating, by 97.4 % for the AlCrN coating and the heat-treated sample exhibited 74.1 % lower wear compared to as-casted H13 tool steel.

The coefficient of friction (CoF) of the TiN coatings was significantly improved compared to the other samples. The CoF was reduced by 72.8 % for TiN coating, by 11.3 % for the AlCrN coating and the heat-treated sample exhibited 9.1 % lower CoF compared to as-casted H13 tool steel.

## References


[1] D. Dinesh Kumar, R. Rani, N. Kumar, K. Panda, A.M. Kamalan Kirubaharan, P. Kuppusami, R. Baskaran, Tribochemistry of TaN, TiAlN and TaAlN coatings under ambient atmosphere and high-vacuum sliding conditions, Applied Surface Science, Vol. 499, 2020, Paper 143989, DOI: 10.1016/j.apsusc.2019.143989

[2] J. Wang, M. Zhang, S. Dai, L. Zhu, Research progress in electrospark deposition coatings on titanium alloy surfaces: A short review, Coatings, Vol. 13, No. 8, 2023, Paper 1473, DOI: 10.3390/coatings13081473

[3] Ş. Bayraktar, F. Afyon, Machinability properties of Al-7Si, Al-7Si-4Zn and Al-7Si-4Zn-3Cu alloys, Journal of the Brazilian Society of Mechanical Sciences and Engineering, Vol. 42, No. 4, 2020, Paper 187, DOI: 10.1007/s40430-020-02281-x

[4] H. Coldwell, R. Woods, M. Paul, P. Koshy, R. Dewes, D. Aspinwall, Rapid machining of hardened AISI H13 and D2 moulds, dies and press tools, Journal of Materials Processing Technology, Vol. 135, No. 2-3, 2003, pp. 301-311, DOI: 10.1016/S0924-0136(02)00861-0

[5] W.R. Prudente, J.F.C. Lins, R.P. Siqueira, P.S.N. Mendes, R.E. Pereira, Microstructural evolution under tempering heat treatment in AISI H13 hot-work tool steel, International Journal of Engineering Research and Applications, Vol. 7, No. 4, 2017, pp. 67-71, DOI: 10.9790/9622-0704046771

[6] G. Wang, J. Zhang, R. Shu, S. Yang, High temperature wear resistance and thermal fatigue behavior of Stellite-6/WC coatings produced by laser cladding with Co-coated WC powder, International Journal of Refractory Metals and Hard Materials, Vol. 81, 2019, pp. 63-70, DOI: 10.1016/j.ijrmhm.2019.02.024

[7] H. Khalid Rafi, G.D. Janaki Ram, G. Phanikumar, K. Prasad Rao, Microstructural evolution during friction surfacing of tool steel H13, Materials & Design, Vol. 32, No. 1, 2011, pp. 82-87, DOI: 10.1016/j.matdes.2010.06.031

[8] M. Yu, R. Shivpuri, R.A. Rapp, Effects of molten aluminum on H13 dies and coatings, Journal of Materials Engineering and Performance, Vol. 4, No. 2, 1995, pp. 175-181, DOI: 10.1007/BF02664111

[9] A. Lakshman Kumar, R. Vignesh, Experimental study on mechanical and tribological properties of H13 tool steel using liquid nitriding, Middle-East Journal of Scientific Research, Vol. 24, No. S1, 2016, pp. 291-295, DOI: 10.5829/idosi.mejsr.2016.24.S1.60

[10] R.D. Torres, P.C. Soares Jr., C. Schmitz, C.J.M. Siqueira, Influence of the nitriding and TiAlN/TiN coating thickness on the sliding wear behavior of duplex treated AISI H13 steel, Surface and Coatings Technology, Vol. 205, No. 5, 2010, pp. 1381-1385, DOI: 10.1016/j.surfcoat.2010.07.102

[11] L. García González, J. Hernández Torres, M.G. Garnica Romo, L. Zamora Peredo, A.M. Courrech Arias, E. León Sarabia, F.J. Espinoza Beltrán, Ti/TiSiNO multilayers fabricated by co-sputtering, Journal of Materials Engineering and Performance, Vol. 22, No. 8, 2013, pp. 2377-2381, DOI: 10.1007/s11665-013-0523-1

[12] J. Kovacich, D. Harwig, A. Endemann, Metallographic and extraction replica methods for characterization of tungsten heavy alloy: H13 clads, Metallography, Microstructure, and Analysis, Vol. 13, No. 3, 2024, pp. 452-461, DOI: 10.1007/s13632-024-01067-0

[13] R.C. Touhami, S. Mechachti, K. Bouhamla, A. Hadji, A. Khettache, Wear behavior and microstructure changes of a high chromium cast iron: The combined effect of heat treatment and alloying elements, Metallography, Microstructure, and Analysis, Vol. 12, No. 4, 2023, pp. 580-590, DOI: 10.1007/s13632-023-00976-w

[14] H. Khalid Rafi, G.D. Janaki Ram, G. Phanikumar, K. Prasad Rao, Friction surfaced tool steel (H13) coatings on low carbon steel: A study on the effects of process parameters on coating characteristics and integrity, Surface and Coatings Technology, Vol. 205, No. 1, 2010, pp. 232-242, DOI: 10.1016/j.surfcoat.2010.06.052

[15] M. Alphonse, V.K. Bupesh Raja, M. Gupta, Effect of coating type on tribological response of H13 tool steel, Surface Review and Letters, Vol. 29, No. 6, 2022, Paper 2250074, DOI: 10.1142/S0218625X22500743

[16] W.H. Kan, L. Chang, The mechanisms behind the tribological behaviour of polymer matrix composites reinforced with $TiO_2$ nanoparticles, Wear, Vol. 474-475, 2021, Paper 203754, DOI: 10.1016/j.wear.2021.203754

[17] K. Mao, D. Greenwood, R. Ramakrishnan, V. Goodship, C. Shrouti, D. Chetwynd, P. Langlois, The wear resistance improvement of fibre reinforced polymer composite gears, Wear, Vol. 426-427, No. B, 2019, pp. 1033-1039, DOI: 10.1016/j.wear.2018.12.043

[18] E. Ura-Bińczyk, K. Kulikowski, W. Chromiński, J. Smolik, M. Lewandowska, Microstructure and properties of AlCr and AlCrFe coatings deposited by magnetron sputtering, Archives of Civil and Mechanical Engineering, Vol. 23, No. 2, 2023, Paper 140, DOI: 10.1007/s43452-023-00681-z

[19] G. Telasang, J. Dutta Majumdar, G. Padmanabham, I. Manna, Wear and corrosion behavior of laser surface engineered AISI H13 hot working tool steel, Surface and Coatings Technology, Vol. 261, 2015, pp. 69-78, DOI: 10.1016/j.surfcoat.2014.11.058

[20] V. Chayeuski, V. Zhylinski, V. Kazachenko, A. Tarasevich, A. Taleb, Structural and mechanical properties of DLC/TiN coatings on carbide for wood-cutting applications, Coatings, Vol. 13, No. 7, 2023, Paper 1192, DOI: 10.3390/coatings13071192

[21] I.S. Vinoth, S. Detwal, V. Umasankar, A. Sarma, Tribological studies of automotive piston ring by diamond-like carbon coating, Tribology – Materials, Surfaces & Interfaces, Vol. 13, No. 1, 2019, pp. 31-38, DOI: 10.1080/17515831.2019.1569852

[22] S.K. Mishra, S. Ghosh, S. Aravindan, Investigations into friction and wear behavior of AlTiN and AlCrN coatings deposited on laser textured WC/Co using novel open tribometer tests, Surface and Coatings Technology, Vol. 387, 2020, Paper 125513, DOI: 10.1016/j.surfcoat.2020.125513

[23] R. Arrabal, M. Mohedano, E. Matykina, A. Pardo, B. Mingo, M.C. Merino, Characterization and wear behaviour of PEO coatings on 6082-T6 aluminium alloy with incorporated α-$Al_2O_3$ particles, Surface and Coatings Technology, Vol. 269, 2015, pp. 64-73, DOI: 10.1016/j.surfcoat.2014.10.048

[24] J. Yi, Y. Xu, Z. Liu, L. Xiao, Effect of TiC content and TaC addition in substrates on properties and wear behavior of TiAlN-coated tools, Coatings, Vol. 12, No. 12, 2022, Paper 1911, DOI: 10.3390/coatings12121911

[25] M. Husain, N. Haldar, L.K. Meena, M. Ghosh, Evaluation of microstructure, mechanical properties, wear resistance and corrosion behaviour of friction stir-processed AZ31B-H24 magnesium alloy, Metallography, Microstructure, and Analysis, Vol. 12, No. 1, 2023, pp. 34-48, DOI: 10.1007/s13632-023-00933-7

[26] W.A. Waleed, A. Chathriyan, R. Sam Singh Vimal, Experimental investigation on the influence of process parameters in thermal drilling of metal matrix composites, FME Transactions, Vol. 46, No. 2, 2018, pp. 171-176, DOI: 10.5937/fmet1802171W

[27] V.C. Uvaraja, N. Natarajan, Optimization on friction and wear process parameters using Taguchi technique, International Journal of Engineering and Technology, Vol. 2, No. 4, 2012, pp. 694-699.
[28] N. Kaushik, S. Singhal, Examination of wear properties in dry-sliding states of SIC strengthened Al-alloy metal matrix composites by using Taguchi optimization approach, International Journal of Applied Engineering, Research, Vol. 12, No. 20, 2017, pp. 9708-9716.
[29] A.V. Maksimkin, V.D. Danilov, F.S. Senatov, L.K. Olifirov, S.D. Kaloshkin, Wear performance of bulk oriented nanocomposites UHMWPE/FMWCNT and metal-polymer composite sliding bearings, Wear, Vol. 392-393, 2017, pp. 167-173, DOI: 10.1016/j.wear.2017.09.025
[30] J. Qu, P.J. Blau, A new model to calculate friction coefficients and shear stresses in thermal drilling, Journal of Manufacturing Science and Engineering, Vol. 130, No. 1, 2008, Paper 014502, DOI: 10.1115/1.2815341